A Revised Architecture of Primary Cell Walls Based on Biomechanical Changes Induced by Substrate-Specific Endoglucanases[1][C][W][OA]

Yong Bum Park and Daniel J. Cosgrove*

Department of Biology, Pennsylvania State University, University Park, Pennsylvania 16802

Xyloglucan is widely believed to function as a tether between cellulose microfibrils in the primary cell wall, limiting cell enlargement by restricting the ability of microfibrils to separate laterally. To test the biomechanical predictions of this "tethered network" model, we assessed the ability of cucumber (*Cucumis sativus*) hypocotyl walls to undergo creep (long-term, irreversible extension) in response to three family-12 endo-β-1,4-glucanases that can specifically hydrolyze xyloglucan, cellulose, or both. Xyloglucan-specific endoglucanase (XEG from *Aspergillus aculeatus*) failed to induce cell wall creep, whereas an endoglucanase that hydrolyzes both xyloglucan and cellulose (Cel12A from *Hypocrea jecorina*) induced a high creep rate. A cellulose-specific endoglucanase (CEG from *Aspergillus niger*) did not cause cell wall creep, either by itself or in combination with XEG. Tests with additional enzymes, including a family-5 endoglucanase, confirmed the conclusion that to cause creep, endoglucanases must cut both xyloglucan and cellulose. Similar results were obtained with measurements of elastic and plastic compliance. Both XEG and Cel12A hydrolyzed xyloglucan in intact walls, but Cel12A could hydrolyze a minor xyloglucan compartment recalcitrant to XEG digestion. Xyloglucan involvement in these enzyme responses was confirmed by experiments with Arabidopsis (*Arabidopsis thaliana*) hypocotyls, where Cel12A induced creep in wild-type but not in xyloglucan-deficient (*xxt1/xxt2*) walls. Our results are incompatible with the common depiction of xyloglucan as a load-bearing tether spanning the 20- to 40-nm spacing between cellulose microfibrils, but they do implicate a minor xyloglucan component in wall mechanics. The structurally important xyloglucan may be located in limited regions of tight contact between microfibrils.

Since the 1970s, xyloglucan (XyG) has been a central figure in theories relating primary cell wall architecture to plant cell enlargement (Keegstra et al., 1973; Labavitch and Ray, 1974; Hayashi, 1989). As the major physical restraint to cell expansion, the primary cell wall plays a pivotal role in cell growth, morphogenesis, and tissue mechanics (Cosgrove, 2005; Schopfer, 2006; Hamant and Traas, 2010). Understanding of cell wall architecture is a cornerstone for conceiving the possible molecular mechanisms by which plant cells modify their walls to control growth as well as influence cell mechanics, water relations, and other properties. Although the biochemical structures of cell wall polymers are well established (Harris and Stone, 2008; Caffall and Mohnen, 2009; Albersheim et al., 2011; Burton et al., 2010; Scheller and Ulvskov, 2010), less certain are their conformations in the wall and their interactions to make a functional network with high tensile strength, resilience, and ability to expand in surface area. Most current depictions of primary cell walls show XyG in an extended conformation, coating the surface of well-separated cellulose microfibrils and spanning the 20- to 40-nm distance between adjacent microfibrils (Somerville et al., 2004; Cosgrove, 2005; Albersheim et al., 2011; Doblin et al., 2010; Fig. 1). Pauly et al. (1999) operationally identified three XyG domains: a xyloglucanase-accessible domain that includes the hypothetical tethers, loops, and free strands between microfibrils; a second domain tightly bound to the surface of cellulose microfibrils (defined as KOH soluble but inaccessible to xyloglucanase); and a third XyG domain only released upon complete wall digestion and thought to be trapped inside or between cellulose microfibrils. This "tethered network model" is based on numerous, but indirect, results, including the extractability and binding behavior of XyG as well as microscopy indicating that XyG is present in the spaces between microfibrils (Hayashi and Maclachlan, 1984; Hayashi et al., 1987; McCann et al., 1990; Pauly et al., 1999). The concept has been illustrated by a variety of cartoons that vary in complexity and detail and typically show pectic polysaccharides as an independent, coextensive phase embedding the cellulose-XyG network.

As noted by Scheller and Ulvskov (2010), "cell wall models that are created to illustrate how wall polymers

[1] This work was supported as part of The Center for LignoCellulose Structure and Formation, an Energy Frontier Research Center funded by the U.S. Department of Energy, Office of Science, and Office of Basic Energy Sciences (award no. DE–SC0001090).

* Corresponding author; e-mail dcosgrove@psu.edu.

The author responsible for distribution of materials integral to the findings presented in this article in accordance with the policy described in the Instructions for Authors (www.plantphysiol.org) is: Daniel J. Cosgrove (dcosgrove@psu.edu).

[C] Some figures in this article are displayed in color online but in black and white in the print edition.

[W] The online version of this article contains Web-only data.

[OA] Open Access articles can be viewed online without a subscription.

www.plantphysiol.org/cgi/doi/10.1104/pp.111.192880

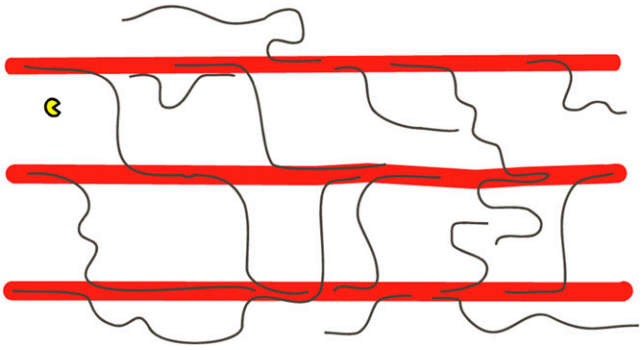

Figure 1. Cartoon of the tethered network model of the primary cell wall, in which xyloglucans (thin strands) bind to the surface of cellulose microfibrils (thick rods), forming a load-bearing network (redrawn after Albersheim et al. [2011] and Pauly et al. [1999]). The semicircle (top left) represents the approximate size of a family-12 endoglucanase used in this study, assuming microfibrils with 20-nm spacing. The microfibrils and the xyloglucan would be longer than what is represented here. [See online article for color version of this figure.]

are organized in higher-order structures influence the thinking about biological functions of the hemicelluloses." Thus, any molecular model of the primary cell wall leads to predictions and expectations about how it will respond to mechanical forces, what kinds of enzymes and biochemical processes might be involved in its expansive growth, and how new polymers could be integrated into its structure. The tethered network model inevitably emphasizes the hypothetical XyG tethers between microfibrils as key determinants of cell wall mechanics and as points for control of cell wall expansion. Although this model is widely accepted, the biomechanical evidence in support of XyG tethers is indirect and open to alternative interpretations. Moreover, some experimental results seem at odds with its predictions (e.g. the failure of XyG endohydrolase/transglucosylase to induce significant cell wall creep comparable to expansin's action [McQueen-Mason et al., 1993; Saladié et al., 2006] and the near-normal phenotype of a XyG-deficient Arabidopsis [*Arabidopsis thaliana*] mutant [Cavalier et al., 2008; Park and Cosgrove, 2012]). Moreover, NMR studies have not detected the extensive XyG-cellulose interactions proposed in the model (Bootten et al., 2004; Dick-Pérez et al., 2011), and neutral pectins have been shown to bind to cellulose in vitro, potentially functioning as tethers in parallel with XyG (Zykwinska et al., 2005). Thus, there are good grounds for reexamining the role of XyG in cell wall mechanics.

In this study, we tested the biomechanical predictions of the tethered network model. For our approach, we digested primary walls with endoglucanases that differ in their substrate specificities and measured the mechanical consequences with assays of cell wall creep and mechanical compliance. This is related to the approach originally used to identify expansins (McQueen-Mason et al., 1992) and provides a direct assessment of the structural role of specific wall polymers. We reasoned that if cellulose microfibrils were connected primarily by XyG tethers, as depicted in Figure 1, digestion of the enzyme-accessible XyG between microfibrils should provoke wall extension and mechanical weakening. The results proved contrary to these predictions, instead pointing to a minor, relatively inaccessible XyG-cellulose structure with importance in cell wall mechanics and with consequences for models of cell wall architecture and mechanisms of cell wall loosening.

RESULTS

Distinctive Actions of Family-12 Endoglucanases

For initial experiments, we made use of three endo-β-1,4-glucanases from glycosyl hydrolase family 12 (www.cazy.org). The advantage of this approach is that the enzymes have similar structures and enzymatic mechanisms (Sandgren et al., 2005), so differences in wall action are more likely to be due to substrate specificity than to differences in the size or shape of the protein. The enzymes are small one-domain proteins (25 kD, approximately 4 nm in diameter), lack a separate carbohydrate-binding domain, and differ in substrate specificities. Their size is below the porosity limit of primary cell walls (Carpita et al., 1979; Baron-Epel et al., 1988) and less than the spacing between cellulose microfibrils, so they should have access to polysaccharides in the hydrated matrix between microfibrils (e.g. the hypothesized XyG tethers). One enzyme was XEG, the XyG-specific endoglucanase, or "xyloglucanase," from *Aspergillus aculeatus* used by Pauly et al. (1999) to define the enzyme-accessible tethers, loops, and free strands of XyG between cellulose microfibrils. The second enzyme, Cel12A from *Hypocrea jecorina*, digests both XyG and cellulose (Yuan et al., 2001; Karlsson et al., 2002). The third enzyme, CEG from *Aspergillus niger*, is a cellulose-specific endoglucanase, or "cellulase," according to the supplier (www.megazyme.org). We first tested the substrate specificity of these enzymes with XyG and cellulose substrates, confirming that XEG indeed hydrolyzed XyGs but not cellulose, CEG hydrolyzed cellulose but not XyG, and Cel12A possessed both activities (Fig. 2). We also tested the three enzymes for hydrolytic activities against the other major wall polysaccharides (other than glucans), but the activities were negligible (Supplemental Fig. S1).

To test their ability to induce cell wall creep, we added the enzymes individually to the solution surrounding cell wall specimens clamped in a constant-force extensometer (Cosgrove, 1989; Yuan et al., 2001). The wall specimens were prepared from growing cucumber (*Cucumis sativus*) hypocotyls briefly heated to inactivate endogenous wall-loosening activities and lightly abraded to promote rapid enzyme penetration through the cuticle. Based on the tethered network model, we expected XEG and Cel12A to induce creep, assuming that they could access the XyG tethers between microfibrils. At 0.1 μg mL^{-1}, Cel12A indeed

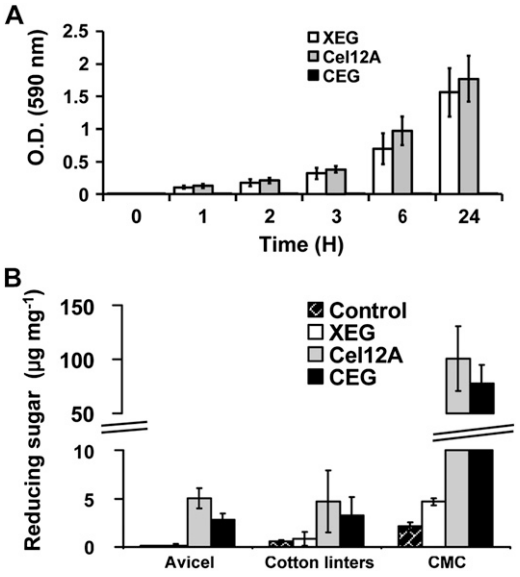

Figure 2. Hydrolytic activities of family-12 endoglucanases. A, Time course for hydrolysis of azurine cross-linked XyG. Hydrolysis by CEG was not detected. O.D., Optical density. B, Comparison of the hydrolysis of different forms of celluloses as measured by the release of reducing sugars. CMC, Carboxymethyl cellulose. Error bars show 95% confidence intervals ($\pm 1.96 \times$ SE; $n = 3$).

induced a high creep rate (Fig. 3A), confirming a previous report (Yuan et al., 2001). However, XEG was totally ineffective, even at 1,000 times greater concentration (Fig. 3B). This was unexpected. Likewise, CEG was ineffective (as expected).

As XEG and Cel12A were able to digest XyG in the cucumber walls (see below), the lack of wall extension by XEG indicated that hydrolysis of enzyme-accessible XyG tethers was not sufficient to loosen the wall, whereas the positive result with Cel12A, combined with the negative result with CEG, suggested that digestion of both XyG and an unbranched β-1,4-D-glucan (cellulose) was required for endoglucanase-induced creep. We tested this idea by simultaneous treatment with XEG and CEG (Fig. 3C); at 10 μg mL^{-1}, the combined enzymes had no effect on creep, and at 100 μg mL^{-1}, the combination induced a very small creep rate, which was negligible compared with that induced by 1,000 times less Cel12A. Thus, simultaneous digestion of XyG and cellulose by separate enzymes was unable to mimic the creep effect of Cel12A. In other experiments, we found that simultaneous treatment with CEG reduced the effectiveness of Cel12A (Fig. 3D), suggesting the CEG nonproductively occupied a site that Cel12A could digest and thereby induce wall creep.

These enigmatic results suggested various possible explanations: (1) Cel12A might digest some other structural (nonglucan) component of the wall. We found no evidence to support this possibility from assays with a range of cell wall polysaccharides (Supplemental Fig. S1). (2) XEG access to interfibrillar XyG might be blocked by pectins (Marcus et al., 2008; Zhao et al., 2008). This seemed unlikely in view of the strong effect of Cel12A, but we tested this idea directly by pretreating the wall with pectate lyase and the calcium chelator cyclohexane diamine tetraacetic acid (CDTA) to reduce the postulated blockage by pectin. These pretreatments transiently weakened the wall, but XEG still did not cause creep (Fig. 4), so we reject this explanation. (3) The hypothetical XyG tethers might assume an unusual conformation or packing that XEG cannot digest, but it is digestible by Cel12A. (4) The hypothetical connection between microfibrils might be

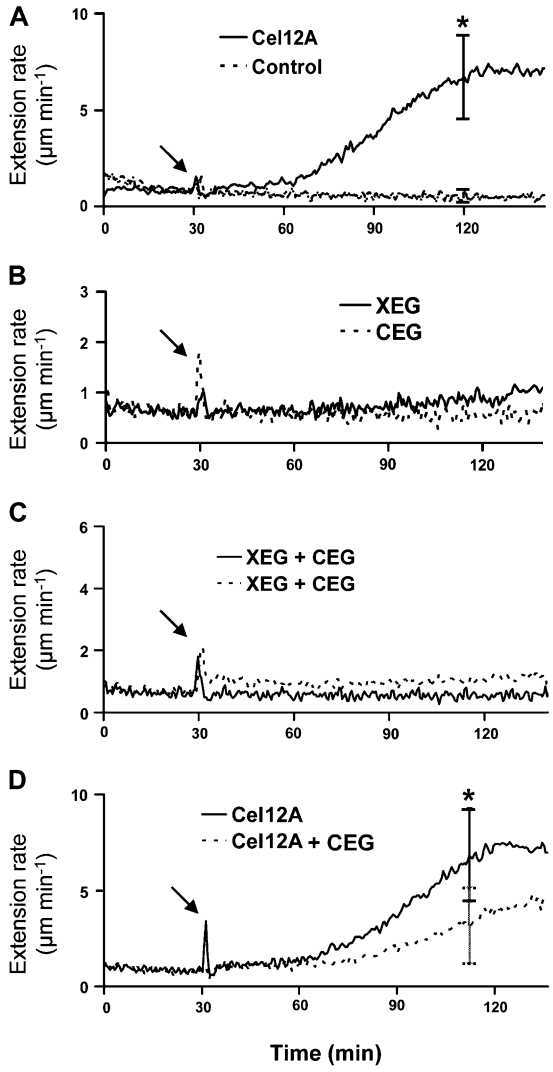

Figure 3. Wall extension induced by family-12 endoglucanases. These curves are averages of six to 19 responses. Arrows indicate when enzyme was added; the spike at this point is a mechanical artifact due to buffer exchange. No enzyme was added in the control. A, Wall creep induced by Cel12A (0.1 μg mL^{-1}; $13 \leq n \leq 15$). B, Wall creep was not induced by XEG or CEG (each 100 μg mL^{-1}; $13 \leq n \leq 19$). C, Wall creep was not induced by XEG + CEG mixtures ($8 \leq n \leq 11$). D, Wall extension induced by Cel12A (0.1 μg mL^{-1}) alone and by Cel12A (0.1 μg mL^{-1}) + CEG (10 μg mL^{-1}; $n = 6$). Error bars show 95% confidence intervals. * $P < 0.05$ in t test comparison of means at selected time points.

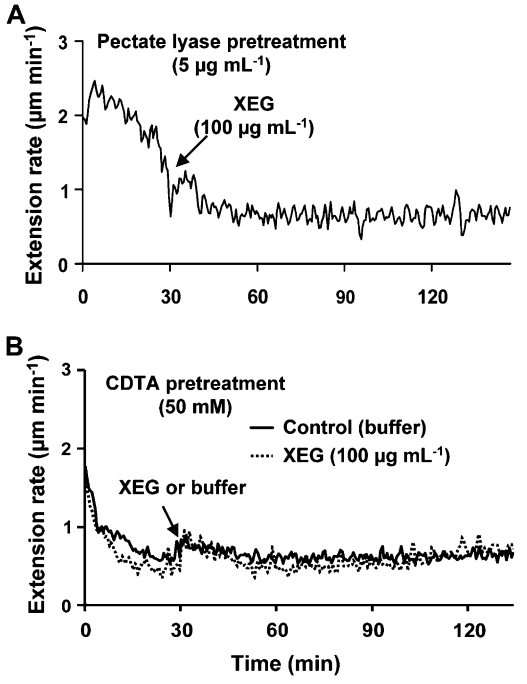

Figure 4. Wall-creep responses to XEG are not sensitized by pectin-disrupting pretreatments. A, Walls predigested with pectate lyase (initial 30 min) followed by XEG (mean of 10 curves). B, Walls preincubated in 50 mM CDTA (pH 6.5) for the first 30 min followed by XEG (average of 12 responses). The control included CDTA pretreatment but not XEG.

an amalgam of XyG and cellulose, whose efficient digestion requires one enzyme with both activities (i.e. separate enzymes would be ineffective due to the need to alternatively and repeatedly hydrolyze the two intertwined polymers).

To test possibilities 3 and 4, we assayed two additional endoglucanases with xyloglucanase and cellulase activities: BlXG12, a family-12 enzyme from *Bacillus licheniformis*, and PpXG5, a family-5 enzyme from *Paenibacillus pabuli* (Gloster et al., 2007). Our tests showed that the enzymes possessed both xyloglucanase and cellulase activities (Supplemental Fig. S2) and that both enzymes induced cell wall creep (Fig. 5), although with different lag times that depend on the concentration and effectiveness of the enzymes (Supplemental Fig. S3; Yuan et al., 2001). We also tested AnXEG, a family-12 enzyme from *Aspergillus nidulans* that hydrolyzes XyG but not cellulose (Bauer et al., 2006). Like the XEG from *A. aculeatus*, AnXEG was ineffective in creep assays (Fig. 5). These results show that the creep activity of Cel12A is not unique to that enzyme and support hypothesis 4, that endoglucanase-induced creep requires an enzyme able to digest both XyG and cellulose. They also undercut hypothesis 3, because it is unlikely that an unusual conformational variant of XyG would be substrate for both Cel12A and the nonhomologous family-5 enzyme (PpXG5), which have different structures and substrate-binding grooves (Sandgren et al., 2005; Gloster et al., 2007), yet would not be digested by two family-12 xyloglucanases homologous to Cel12A.

Additional results confirming the involvement of XyG in Cel12A-induced creep came from parallel experiments with walls from an Arabidopsis mutant (*xxt1/xxt2*) lacking XyG (Cavalier et al., 2008). The walls of this mutant should lack the hypothetical XyG-cellulose structure that is digested by Cel12A to induce creep. Therefore, we tested the wall-creep activity of Cel12A using hypocotyl walls from wild-type and *xxt1/xxt2* Arabidopsis. With wild-type walls, Cel12A induced creep very similar to its action on cucumber walls, whereas no creep response was detected with walls from the *xxt1/xxt2* mutant (Fig. 6A). Additionally, XEG did not cause cell wall creep in the wild-type Arabidopsis walls, similar to the results with cucumber walls (Fig. 6B). These results show that XyG is necessary for endoglucanase-induced creep, and they provide additional support for the concept of a XyG-cellulose structure digested by Cel12A but recalcitrant to XEG.

Endoglucanase Effects on Cell Wall Compliance and Artificial Cellulosic Composites

We extended the foregoing results with additional experiments to assess the effects of family-12 endoglucanases on the mechanical compliance of cucumber hypocotyl walls. For these measurements, the walls were predigested with enzyme for 1 h and then extended in two cycles (Cosgrove, 1989). The slope (Δlength/Δforce) of the second extension yields a measure of the elastic (reversible) compliance, whereas the plastic compliance is calculated from the difference between the first and second extensions. As shown in Figure 7, Cel12A at 0.1 μg mL^{-1} increased the plastic compliance by 70% and the elastic compliance by 30% compared with the control, but no significant changes were found after digestion with XEG or CEG, even at

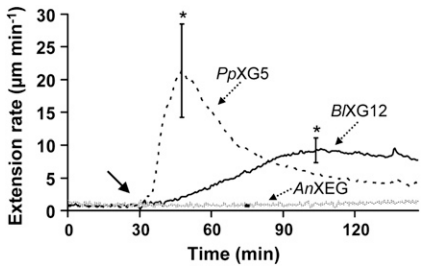

Figure 5. Wall-creep responses to family-5 and family-12 endoglucanases (means of eight to 10 responses). PpXG5 and BlXG12 have both cellulase and xyloglucanase activities, whereas AnXEG (family 12) has xyloglucanase but not cellulase activity. The solid arrow indicates when the enzymes (30 μg mL^{-1}) were added. Error bars show 95% confidence intervals (for AnXEG, the bar is smaller than the line width). * $P <$ 0.05 by Student's two-tailed t test for difference before and after enzyme treatment.

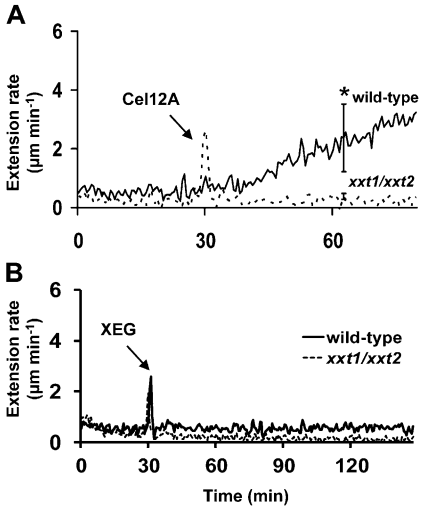

Figure 6. Creep responses of etiolated Arabidopsis wild-type (ecotype Columbia) and XyG-deficient mutant (*xxt1/xxt2*) hypocotyl walls to Cel12A and XEG treatment (average values of seven to eight responses). A, Creep responses to Cel12A. The arrow indicates when Cel12A (1 μg mL^{-1}) was added. Error bars show 95% confidence intervals. * $P < 0.05$ for *t* test comparison of the two treatments at the time indicated. B, Creep responses to XEG. The arrow indicates when XEG (10 μg mL^{-1}) was added.

1,000 times higher concentrations. These results parallel the effects seen in creep assays and indicate that the particular XyG-cellulose structure digested by Cel12A is a determinant of cell wall mechanics as well as enzyme-induced creep, whereas the XEG-accessible XyG has a negligible impact on wall mechanics, at least as measured by creep and stress/strain methods.

To gain further insight into the wall-loosening action of these enzymes, we turned to cellulosic networks ("pellicles") produced by cultures of *Gluconacetobacter xylinus* (formerly *Acetobacter xylinus*). Pellicles can be produced in the presence of XyG or other matrix polysaccharides, which get incorporated to form composites that have been considered analogs of plant cell walls (Chanliaud et al., 2002, 2004). We first tested the effect of the three family-12 enzymes on pure cellulosic pellicles (no polysaccharide additives) in creep assays (Fig. 8A). Both CEG and Cel12A induced creep, followed by breakage after approximately 1 h (3%–4% extension), whereas XEG was ineffective. These results are consistent with cellulose friction and entanglements determining the rheology of such networks (Chanliaud et al., 2002).

With cellulosic composites produced in the presence of 0.5% tamarind (*Tamarindus indica*) XyG, Cel12A still induced a high creep rate, but the response to CEG was greatly diminished (Fig. 8B). XEG also induced a substantial creep rate in the XyG composite, unlike its effect on plant cell walls. These results indicate that direct cellulose entanglements are less limiting for creep for this XyG-containing material compared with the pure cellulosic composite, most likely as a result of the large-scale ordering of microfibrils in the XyG-containing composite (Chanliaud et al., 2002; Whitney et al., 2006). The XEG result is also consistent with XyG cross-linking of the bacterial composite but stands in stark contrast to the result obtained with plant cell walls. We conclude that XyG in the bacterial composite does not closely mimic its structural role in native plant cell walls.

Evidence for a Special XyG Component Accessible to Cel12A

To verify that XyG in the cucumber wall was accessible to XEG and Cel12A, as well as to look for structural differences in the corresponding XyGs, we treated whole walls with XEG or Cel12A and measured the released xyloglucan oligosaccharides (XGOs) through high-performance anion-exchange chromatography-pulsed amperometric detection (HPAEC-PAD) analysis. At an enzyme loading of 10 μg mL^{-1}, Cel12A released about 40% more XGOs than XEG did, but the profiles of XGOs were similar (Fig. 9A). The quantitative difference between the two enzymes was not sufficient to account for their different effects on cell wall mechanics. The main XGOs liberated by the two enzymes were XXXG and XXFG (using the shorthand for XGOs proposed by Fry et al. [1993]). Smaller amounts of XXG, XXGG, XLFG, and other XGOs were also released. This XGO pattern is similar to that reported for primary cell walls of other dicots (Pauly et al., 1999; Hsieh and Harris, 2009). The similarity in XGO patterns indicates the XyGs targeted by the two enzymes were structurally similar.

To examine this last point in further detail, we sequentially digested and extracted the cucumber walls with XEG, Cel12A, 4 M NaOH, and finally a cellulase that completely solubilized the residue (endoglucanase I from Megazyme). These sequential fractions corresponded to 50%, 8%, 33%, and 9% of the total XyG in the wall (Supplemental Fig. S4A); only minor differences in the XGO profiles were seen in these fractions (Supplemental Fig. S4, B and C), indicating only subtle differences in XyG structure in these various compartments. We also detected cello-oligosaccharides in the Cel12A digest but not in the XEG digest (Supplemental Fig.

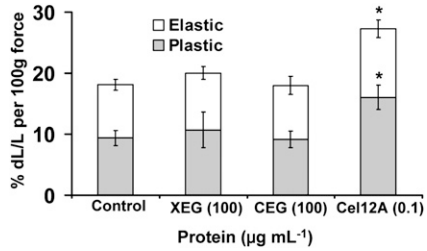

Figure 7. Alteration of wall compliance by family-12 enzyme treatment. Error bars show 95% confidence intervals ($10 \leq n \leq 12$). * $P <$ 0.05 by Student's two-tailed *t* test for difference from buffer control.

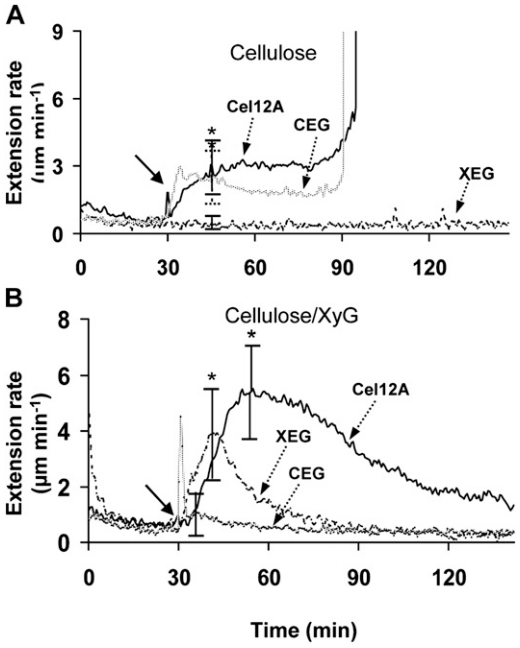

Figure 8. Creep responses of bacterial cellulose and cellulose/XyG composites to family-12 enzymes (average values of eight to 10 responses). Solid arrows indicate when enzymes were added. A, Creep induced in bacterial cellulose pellicle by Cel12A (3 μg mL^{-1}), XEG (100 μg mL^{-1}), and CEG (30 μg mL^{-1}) in 20 mM sodium acetate (pH 5.0) with 15 g of force. Error bars show 95% confidence intervals. * $P <$ 0.05 by Student's two-tailed *t* test for before and after enzyme treatment. For Ce112A and CEG treatments, half the samples broke at approximately 90 to 120 min, while the other half continued to creep at diminished rates. B, Creep of cellulose-XyG composite in response to Cel12A (3 μg mL^{-1}), XEG (100 μg mL^{-1}), and CEG (100 μg mL^{-1}) in 20 mM sodium acetate (pH 5.0) with 7.5 g of force. Error bars show 95% confidence intervals. * $P < 0.05$ by Student's two-tailed *t* test for before and after enzyme treatment.

S4D), consistent with the idea the Cel12A-induced creep involves cellulose digestion.

Figure 9B shows the release of XGOs as a function of XEG and Cel12A concentration. At 0.1 μg mL^{-1}, Cel12A released much more XGO than did XEG. More significantly, the XEG curve reached a plateau at 100 μg mL^{-1}, whereas Cel12A continued to release XGOs, exceeding the amount of XEG-released XGO by approximately 20%. These XGO-release curves support the conclusion that the wall contains a minor XyG compartment that is digestible by Cel12A but not by XEG. This compartment may be identical to the special XyG-cellulose structure detected above in the biomechanics assays. Consistent with this idea, a plot of creep rate as a function of XGOs released by the two enzymes shows that creep rate increased monotonically as XGOs were released by Cel12A, but the XEG curve plateaued (Fig. 9C). To test this idea in yet another way, walls were exhaustively digested with one of these enzymes and washed, and then XGOs released by the other enzyme were assayed. When XEG predigestion was followed by Cel12A, much higher levels of XGOs were released than when the order of the enzyme treatments was reversed (Fig. 9D). These additional results support the idea that Cel12A can digest a XyG compartment that is recalcitrant to XEG.

Finally, we evaluated the total XyG content of cucumber walls by measuring isoprimeverose [xylosyl-α-(1,6)-glucose] after exhaustive digestion with Driselase (Cavalier et al., 2008). Approximately 45% of the XyG was removed from the wall by exhaustive XEG digestion, whereas 55% was removed by Cel12A (Supplemental Fig. S5). Thus, the physical effects of Cel12A are associated with digestion of a XyG compartment that constitutes a minor fraction of the total XyG (maximally 10% [i.e. the difference between 55% and 45%]). In fact, the biomechanical changes induced by Cel12A began at much lower levels of XyG digestion. For instance, at 0.1 μg mL^{-1}, Cel12A digestion increased wall compliance (Fig. 7) and creep rate (Fig. 3) within 1 h. Only 1.5% of the XyG was solubilized by such a treatment (Supplemental Fig. S6), and only one-fifth of this XyG is likely to be load bearing and Cel12A specific (compare with Supplemental Fig. S4A). Thus, the large biomechanical effects caused by Cel12A may be traced to the digestion of a remarkably small fraction (perhaps 0.3%) of the total wall XyG.

DISCUSSION

We used a set of homologous endoglucanases with varying substrate specificities to test the predictions of the tethered network model (Fig. 1), reasoning that digestion of xyloglucanase-accessible XyGs between microfibrils should result in cell wall weakening, which we assayed by creep and stress/strain measurements. The results are at odds with this prediction and thus argue against a major mechanical role for XyG tethers spanning the space between adjacent microfibrils. Instead, our results point to a minor, relatively inaccessible XyG compartment that may be intertwined or otherwise complexed with cellulose, forming a load-bearing connection between microfibrils. These results have implications for cell wall architecture and put constraints on the potential for enzymatic mechanisms of cell wall loosening.

Microfibrils Connected Not by XyG Tethers but a XyG-Cellulose Amalgam

According to current views (Pauly et al., 1999; Albersheim et al., 2011), XyG tethers spanning the 20- to 40-nm distance between adjacent microfibrils (Fig. 1) should be part of the XEG-susceptible domain. We confirmed that XEG indeed digests nearly half of the wall XyG, but without a concomitant change in either the creep behavior or stress/strain responses of the wall. Thus, if XyG tethers exist, they are evidently not significant determinants of the mechanics of these walls, at least by these measures. We note that tether-like strands have been observed in some primary walls

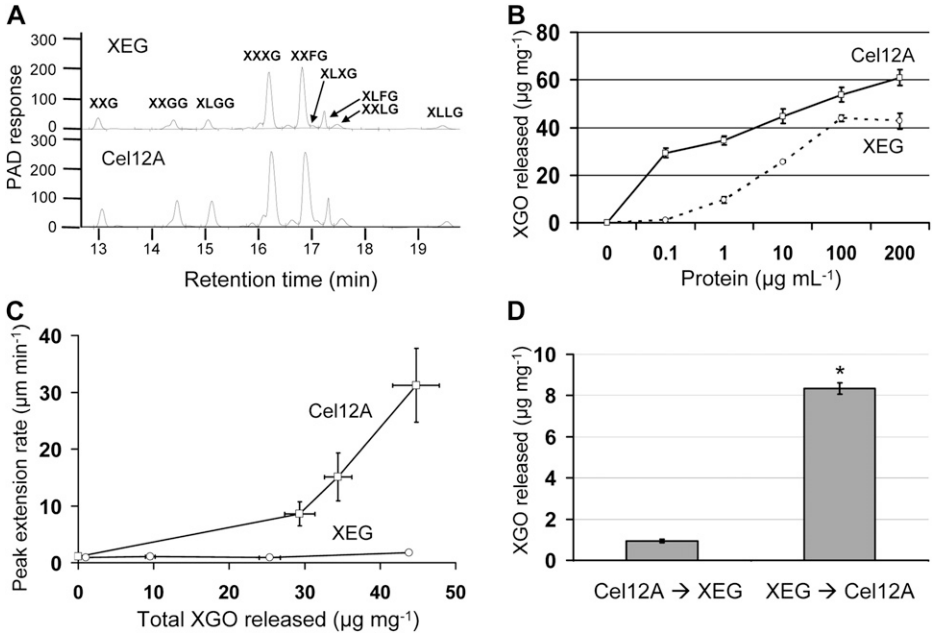

Figure 9. Dionex HPLC analysis of XGOs of cucumber hypocotyls released by Cel12A and XEG. A, HPLC profiles of XGOs released by Cel12A and XEG (10 μg mL^{-1}). B, Total XGOs released as a function of Cel12A and XEG concentration. Error bars show 95% confidence intervals (n = 2). C, Plot of peak wall extension rate against total XGOs released. Error bars show 95% confidence intervals (HPLC, n = 2; wall extension assay, $10 \leq n \leq 19$). D, Amount of XGOs released by XEG or Cel12A following exhaustive predigestion with the other enzyme. Values are given for release by the second enzyme treatment. Error bars show 95% confidence intervals (n = 2). * $P < 0.05$ by Student's two-tailed t test for difference between means.

(McCann et al., 1990; Itoh and Ogawa, 1997) but not in others (Fujino et al., 2000). Moreover, even when they are observed, their contribution to cell wall mechanics is difficult to assess from such images. Our XEG results do not support the tethered network concept, at least for hypocotyl walls from cucumber and Arabidopsis.

The lack of a XEG effect contrasts with the pronounced action of the closely related endoglucanase Cel12A, where we found evidence that a quantitatively minor XyG-cellulose complex contributes to cell wall mechanics. We base this conclusion on the induction of cell wall creep by three endoglucanases that hydrolyze both XyG and cellulose (Cel12A, BlXG12, and PpXG5), whereas no creep effect was seen when walls were treated with a cocktail containing both XEG and CEG, endoglucanases specific for XyG and cellulose, respectively. The involvement of XyG in these responses was further established by use of the XyG-deficient (*xxt1/xxt2*) mutant of Arabidopsis: Cel12A induced creep in the wild-type walls but not in the XyG-deficient walls. These and other results reported here lead us to postulate that endoglucanase-induced wall loosening requires the digestion of a XyG-cellulose complex that links microfibrils together in a distinctive way.

The exact location of the postulated XyG-cellulose complex is uncertain, but the fact that it is not digested by the combination of XEG and CEG suggests that it is located in a relatively inaccessible site and that its hydrolysis requires repeated alternating attacks on XyG and cellulose chains. Otherwise, one would expect that separate attack by the two enzymes would digest the complex. One possible scheme that is consistent with our results is depicted in Figure 10A, where the important XyG is depicted as a one-molecule-thick adhesive between adjacent microfibrils. In this scheme, microfibril adhesion is mediated by lateral, noncovalent bonding by a single XyG layer between two microfibril surfaces. With its ability to digest both cellulose and XyG, Cel12A could digest this "sequestered" XyG, perhaps after an appreciable lag, and the microfibrils would then be freed to move in response to wall stress. Microfibril movement after release would presumably

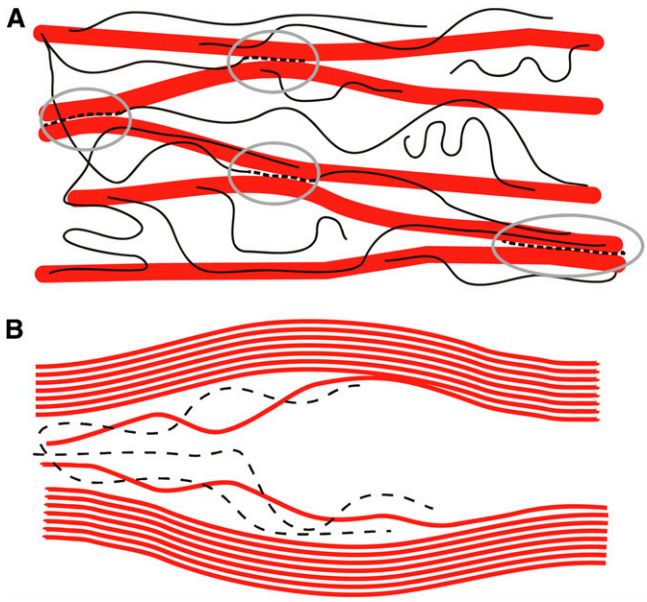

Figure 10. Revised cartoon of primary cell wall architecture. A, The thick rods represent cellulose microfibrils, and the thin lines are XyGs. The load-bearing XyGs are represented as broken lines between microfibrils and are highlighted by the gray circles. They may act as a molecular binder to connect two adjacent microfibrils that are in close contact. The other XyGs are not load bearing and are shown as solid lines. B, A closeup of the hypothetical load-bearing junctions, where XyG is depicted as intertwined with disordered surface glucans from two adjacent microfibrils (at left), effectively sticking the microfibrils together at this point. [See online article for color version of this figure.]

be limited by viscous drag and the entanglement of other matrix polymers surrounding or bound to the microfibril. In this scheme, microfibril bundling, mediated by XyG, would play a key role in wall biomechanics and the responses to Cel12A digestion. The fact that Cel12A increases cell wall compliance (Fig. 7) suggests that it irreversibly reduces the number of such microfibril-microfibril contacts, which we propose are important determinants of primary cell wall mechanics.

A variant scheme is depicted in Figure 10B, where the important XyG at microfibril junctions is pictured as entangled with disordered surface glucans of adjacent microfibrils. The result is a local region of microfibril adhesion that could only be undone by an enzyme with both xyloglucanase and cellulase activities. A variation of this scheme might entail deeper penetration of the XyG into the cellulose microfibrils, resulting in a disordered region that might be prone to adhere to similarly disordered regions of adjacent microfibrils.

This new architecture involves XyG, but not as a gap-spanning tether stretched taut between adjacent microfibrils, as commonly depicted. Instead, a minor fraction of the XyG acts as a microfibril adhesive in the limited places where microfibrils come in sufficiently close contact and a XyG is suitably located to become sandwiched between the two cellulose surfaces, perhaps entangled with surface glucans of the microfibrils. In this scheme, turgor-generated wall stress is not transmitted between microfibrils by the XyG backbone, as envisioned in the tethered network model, but involves numerous lateral interactions proportional to the contact area between cellulose and XyG. Such an architecture might be stronger than the tethered network of Figure 1, where XyG chains are liable to detach from the cellulose surface, one glucan at a time.

This alternative architecture requires regions of close contact (or, more correctly, XyG-mediated contact) between microfibrils. This differs from most current models, where a coating of XyG and other matrix polymers is thought to prevent microfibril contacts (Albersheim et al., 2011). However, there are reasons to suspect that microfibril contacts likely exist. First, scrutiny of cell wall images often reveals potential points of microfibril contact and bundling where these close contacts may occur (Thimm et al., 2000; Ding and Himmel, 2006). Second, NMR studies have concluded that only a small proportion (less than 10%) of the cellulose surface is coated with XyG (Bootten et al., 2004; Dick-Pérez et al., 2011). Third, cell walls (not extracted to remove hemicelluloses) are readily labeled with affinity reagents that bind to cellulose surfaces (e.g. reagents such as the direct cotton dye Pontamine Fast Scarlet 4B [Anderson et al., 2010] and carbohydrate-binding modules that bind crystalline cellulose [Knox, 2008; Lacayo et al., 2010]). Such labeling may indicate unoccupied cellulose surfaces. Fourth, the primary cell wall of the *xxt1/xxt2* mutant, which lacks XyG, maintains most of its functionality (Cavalier et al., 2008; Park and Cosgrove, 2012), which would be unlikely if an essential role of XyG were to coat cellulose surfaces to prevent microfibril coalescence.

Implications for Plant Cell Wall Loosening

These results also have various implications for mechanisms of plant cell wall loosening. First, XyG endotransglucosylase is a plant enzyme that cuts and ligates XyG (Fry et al., 1992; Nishitani and Tominaga, 1992), and in view of Figure 1, it would be expected to loosen the cell wall, leading to cell growth. However, previous tests by creep and stress/strain assays have not confirmed this prediction (McQueen-Mason et al., 1993; Saladié et al., 2006), which is understandable if the enzyme-accessible XyG is not load bearing. By restructuring XyGs in the XEG-accessible domain, the action of this enzyme might result in subtle cell wall changes (Kaku et al., 2004; Van Sandt et al., 2007), but if it cannot access the structurally important XyG-cellulose compartment identified here, its biomechanical actions are likely to be indirect and limited.

Second, we note that Cel12A is not a plant enzyme and that plants lack family-12 glycosyl hydrolases (www.cazy.org). Plant genomes encode glycosyl hydrolases from 34 other enzyme families, two of which (families 9 and 16) may have endo-β-1,4-glucanase activity (Lopez-Casado et al., 2008), but it is unclear whether any of them exert the biomechanical effects of Cel12A. The plant growth effects observed with ectopic expression of plant cellulases may be mediated by a similar mechanism or by some other route (Park et al., 2003; Shani et al., 2004; Hartati et al., 2008). Auxin treatments result in slow increases in wall plastic and elastic compliances (Cleland, 1984), so the cell wall changes caused by Cel12A might be similar to those that occur during long-term auxin-induced growth. Whether this is related to the auxin-induced metabolism of XyG (Labavitch and Ray, 1974; Nishitani and Masuda, 1983; Talbott and Ray, 1992) or to other structural changes in the wall remains to be determined.

Finally, we note that Arabidopsis *xxt1/xxt2* walls are deficient in creep response both to Cel12A (Fig. 6) and to α-expansin (Park and Cosgrove, 2012), suggesting a common target of these two proteins. If this is true, then the XyG-cellulose structure identified here may participate in growth responses mediated by expansins and perhaps other wall-loosening agents.

Our revised model of the cellulose-XyG network resolves serious contradictions of the tethered network model posed by results in this and other studies and suggests that XyG-mediated control of wall extension may be restricted to relatively inaccessible contact surfaces between microfibrils of the primary cell wall. However, this is not the only possible model, and we note some of its limitations. It focuses on the structural and biomechanical architecture of the cellulose-XyG network and does not speak to contributions by other matrix polymers (pectins and arabinoxylans in partic-

ular), which may be important in primary cell walls of different composition, at other developmental states, or for other physical aspects of primary cell wall function. The mechanical tests employed here made use of external uniaxial forces, which do not mimic turgor-generated forces in all respects, and microfibril movements may differ in some aspects. Numerous details of the revised model are not defined, such as the origin, distribution, density, structure, and modification of the biomechanical "hot spots." We offer the revision as a working hypothesis to direct further testing and refinement of our understanding of primary cell walls and how they expand.

MATERIALS AND METHODS

Expression and Purification of Cel12A and AnXEG

Cel12A from *Hypocrea jecorina* was expressed in *Escherichia coli* Tuner (DE3) and purified as described by Yuan et al. (2001). AnXEG from *Aspergillus nidulans* was expressed in *Pichia pastoris*, and purification was performed as described (Cregg et al., 2000; Bauer et al., 2006). The M_r and quality of purified proteins were determined by SDS-PAGE and Coomassie blue staining. CEG from *Aspergillus niger* was purchased from Megazyme (E-CELAN). XEG (from *Aspergillus aculeatus*), PpXG5 (from *Paenibacillus pabuli*), and BlXG12 (from *Bacillus licheniformis*) were obtained from Novozymes. Protein concentrations were quantified by the method of Bradford (1976) or based on supplier data.

Hydrolytic Activities of Endoglucanases

To assess xyloglucanase activity, 10 mg of dye-couple XyG (azurine cross-linked XyG from Megazyme) was mixed with 1 mL of 20 mM sodium acetate (pH 5.0) including 0.1 μg mL^{-1} each enzyme and incubated for 1, 2, 3, 6, and 24 h at 27°C, followed by measurements of optical density at 590 nm. Cellulase activity was measured as release of reducing sugars from cellulose using parahydroxybenzoic acid hydrazine for colorimetric detection (Lever, 1972). Five milligrams of Avicel PH-101 (FMC; no. 9004-34-6), cotton linters (cellulose powder; Fluka; no. 22184), or carboxymethyl cellulose (Sigma; no. C4888) was incubated with 1 μg of enzyme in 1 mL of 20 mM sodium acetate (pH 5.0) at 27°C for 4 h. Enzyme activity against other (nonglucan) polysaccharides was assessed by release of reducing sugars, using various wall polysaccharides as substrate. Two milligrams of polysaccharide was incubated at 27° for 3 h with 1 μg of each endoglucanase in 1 mL of 20 mM sodium acetate (pH 5.0), followed by parahydroxybenzoic acid hydrazine assay. The following polysaccharides were purchased from Megazyme: XyG (tamarind xyloglucan; P-XYGLN), AX (wheat arabinoxylan; P-WAXYL), Ara (sugar beet arabinan; P-ARAB), Gal (lupin galactan; P-GALLU), Man (mannan; P-MANCB), GML (konjac glucomannan low viscosity; P-GLCML), GMH (konjac glucomannan high viscosity; P-GLCMH), GalM (carob galactomannan; P-GALMH), RG (soybean pectic fiber rhamnogalacturonan; P-RHAGN), and PGA (citrus polygalacturonic acid; P-PGACT); polysaccharides from Fluka were X (oat-spelt xylan; 95590) and AP (apple pectin; 76282).

Wall Extension (Creep) Assays

Cucumber (*Cucumis sativus*) and Arabidopsis (*Arabidopsis thaliana*) hypocotyls from 4-d-old etiolated seedlings were collected on ice water, and 1-cm segments were excised from the region immediately below the apical hook and frozen at −80°C as described (Cosgrove, 1989; McQueen-Mason et al., 1992). Cuticles were abraded by rubbing the frozen segments with a carborundum slurry (300-mesh size) to facilitate buffer and protein penetration, and the abraded segments were washed extensively with distilled, deionized water. Cucumber walls were pressed under a weight for 5 min to remove excess water, but no weight was applied to Arabidopsis walls because they were very fragile. Pressed specimens were heat inactivated in boiling water for 15 s (cucumber) or 12 s (Arabidopsis). The wall specimens were clamped (5 mm between clamps) under a constant force of 20 g (cucumber) and 0.5 g (Arabidopsis). The clamped wall segments were incubated with 20 mM sodium acetate (pH 5.0) for 30 min, the incubation buffer was replaced with the same buffer containing enzyme, and wall extension was recorded digitally every 30 s for 2 h (Cosgrove, 1989; Durachko and Cosgrove, 2009). Samples with excessive initial creep rates or showing signs of premature breakage were excluded from analysis (approximately one out of 10 samples). Creep-rate time courses were averaged, and appropriate time points were analyzed for statistical differences. Typical variability in creep responses is illustrated in Supplemental Figure S7, which shows the individual data sets averaged in Figure 3. Wall extension assays, unless otherwise mentioned, were performed with cucumber hypocotyl walls.

Stress/Strain Assays

Heat-inactivated cucumber walls prepared as above were treated with enzyme in 20 mM sodium acetate (pH 5.0) at 27°C for 1 h. The walls were clamped in a custom-made extensometer with 5 mm between clamps and extended at a rate of 3 mm min^{-1} until a force of 20 g was reached; plastic and elastic compliances were calculated from the slopes of the extension/force curves, as described (Cosgrove, 1989; Yuan et al., 2001).

Bacterial Cellulose Composite Preparation and Extension Assay

Gluconacetoacter xylinus (ATGC 53524) was cultured in Hestrin-Schramm medium (Hestrin and Schramm, 1954) containing 2% Glc with or without 0.5% tamarind (*Tamarindus indica*) XyG (Megazyme) at 30°C under static conditions. After 3 d of fermentation, bacterial pellicles (0.23 mm thick) were harvested and washed thoroughly with distilled, deionized water. Cellulose and cellulose/XyG materials were cut into strips (0.55 mm × 0.23 mm in cross-section and 10 mm in length), clamped in a constant force extensometer (5 mm between clamps), and extended with 15 and 7.5 g of force, respectively, with 20 mM sodium acetate (pH 5.0) buffer. Enzymes were added after 30 min.

XGO Analysis

To assess XGOs released by Cel12A and XEG, frozen and thawed cucumber hypocotyl segments (apical 10 mm from eight etiolated hypocotyls; 5 mg dry weight total) were abraded with a carborundum slurry, pressed under a weight for 5 min, heat inactivated in boiling water for 15 s, and incubated with Cel12A or XEG in 100 mM ammonium acetate (pH 5.0) with 0.02% NaN_3 (to inhibit microbial growth) at 27°C for 24 h or for other times as indicated. Supernatant was collected and boiled for 5 min to inactivate the enzymes. For exhaustive XyG digestion, 5 mg (dry weight) of cucumber walls prepared as described above was predigested with one enzyme (XEG or Cel12A; each 100 μg mL^{-1}) in 100 mM ammonium acetate (pH 5.0) with 0.02% NaN_3 at 27°C for 48 h with shaking, washed with distilled, deionized water, boiled in distilled, deionized water for 5 min to inactive the enzymes, and digested with the other enzyme (each 10 μg mL^{-1}) in 100 mM ammonium acetate (pH 5.0) with 0.02% NaN_3 at 27°C for 24 h with shaking. The supernatant was collected and dried under vacuum, and the XGOs were dissolved in 1 mL of 80% ethanol. For sequential XyG digestion, 5 mg (dry weight) of cucumber hypocotyls was prepared as described, heat inactivated, and finely chopped with a razor blade. Chopped walls were incubated in 1 mL of 100 mM ammonium acetate (pH 5.0) with XEG (100 μg mL^{-1}) containing 0.02% NaN_3 at 27°C for 24 h with shaking. The supernatant was collected and dried under vacuum, and XGOs generated by XEG were dissolved in 1 mL of 80% ethanol. The XEG-digested walls were boiled in water for 15 s and incubated in 1 mL of 100 mM ammonium acetate (pH 5.0) with Cel12A (100 μg mL^{-1}) containing 0.02% NaN_3 at 27°C for 24 h with shaking. The supernatant was collected and dried under vacuum, and XGOs (released by Cel12A) were dissolved in 80% ethanol. Cel12A-digested walls were repeatedly digested with Cel12A to confirm complete XyG digestion by Cel12A as described. XyG of Cel12A-digested walls was extracted sequentially three times with 4 M NaOH containing 20 mM $NaBH_4$ for 6, 6, and 12 h at room temperature with shaking. The supernatant containing XyG was neutralized with acetic acid, dialyzed with distilled, deionized water, and dried under vacuum. The XyG solubilized by NaOH extraction was digested with XEG (100 μg mL^{-1}) in 1 mL of 100 mM ammonium acetate (pH 5.0) containing 0.02% NaN_3 at 27°C for 24 h with shaking. Residues of walls extracted with 4 M NaOH were thoroughly washed, neutralized with distilled, deionized water, and incubated with 100 μg mL^{-1} cellulase (endoglucanase I) from *Trichoderma longibrachiatum* (Megazyme;

E-CELTR) in 1 mL of 100 mM ammonium acetate (pH 5.0) containing 0.02% NaN_3 at 37°C for 24 h with shaking. The supernatant was dried under vacuum, and the XGOs (released by cellulase) were dissolved in 80% ethanol. For HPAEC-PAD analysis, XGO-containing samples were centrifuged at 10,000 rpm for 5 min; the supernatants were completely dried, redissolved in distilled, deionized water, and filtered through a 0.22-μm centrifuge filter (Amicon). XGOs were eluted from a Dionex CarboPac PA-200 column at a flow rate of 0.5 mL min^{-1} using a linear gradient over 35 min starting with 0.1 M NaOH to a 0.1 M sodium acetate and 0.1 M NaOH (1:1, v/v) mixture (Park and Cosgrove, 2012). XGOs were detected with a pulsed amperometric detector.

Isoprimeverose Analysis of Cucumber Hypocotyls by Driselase Digestion

Heat-inactivated cucumber hypocotyls (5 mg dry weight) were exhaustively digested with 100 μg of XEG or 100 μg of Cel12A with 1 mL of 100 mM ammonium acetate (pH 5.0) containing 0.02% NaN_3 at 27°C for 48 h with shaking. Nondigested cucumber walls were used for a control. Walls were incubated with 500 μL of 0.5% Driselase (Sigma) in pyridine:acetic acid:water (1:1:98 [pH 4.7]; containing 0.5% chlorobutanol and 0.02% sodium azide) at 37°C for 72 h with shaking as described (Gardner et al., 2002). The Driselase digest was added to 5 volumes of ethanol, incubated at −20°C for 16 h, and centrifuged. The supernatant was dried and resuspended in 500 μL of distilled, deionized water. For HPAEC-PAD analysis, the sample was filtered through a 0.22-μm filter, separated with a Dionex Carbo PA-20 column at 0.5 mL min^{-1} from 0 to 20 min under 125 mM NaOH isocratic conditions, and detected with a pulsed amperometric detector.

Supplemental Data

The following materials are available in the online version of this article.

Supplemental Figure S1. Hydrolytic activity of GH12 enzymes.

Supplemental Figure S2. Hydrolytic activity of GH5 and GH12 endoglucanases.

Supplemental Figure S3. Concentration dependence of creep induced by family-5 and family-12 endoglucanases.

Supplemental Figure S4. Dionex HPLC analysis of sequentially released xyloglucan- and cello-oligosaccharides.

Supplemental Figure S5. Isoprimeverose (IP) released by Driselase digestion.

Supplemental Figure S6. XGOs released by Cel12A.

Supplemental Figure S7. Individual creep curves shown in Fig. 3, A and D.

ACKNOWLEDGMENTS

We thank Mr. Daniel M. Durachko and Mr. Edward R. Wagner (Pennsylvania State University) for their expert technical assistance and Dr. Thomas Richard, Dr. Megan Marshall, Ms. Liza Wilson, and Ms. Jyotsna Pandey (Pennsylvania State University) for their assistance for HPAEC-PAD analysis. We also thank Kirk Matthew Schnorr (Novozymes) for the gift of XEG, PpXG5, and BlXG12.

Received December 22, 2011; accepted February 23, 2012; published February 23, 2012.

LITERATURE CITED

Albersheim P, Darvill A, Roberts K, Sederoff R, Staehelin A (2011) Plant Cell Walls, from Chemistry to Biology. Garland Science, New York, pp 227–272

Anderson CT, Carroll A, Akhmetova L, Somerville C (2010) Real-time imaging of cellulose reorientation during cell wall expansion in Arabidopsis roots. Plant Physiol **152:** 787–796

Baron-Epel O, Gharyal PK, Schindler M (1988) Pectins as mediators of wall porosity in soybean cells. Planta **175:** 389–395

Bauer S, Vasu P, Persson S, Mort AJ, Somerville CR (2006) Development and application of a suite of polysaccharide-degrading enzymes for analyzing plant cell walls. Proc Natl Acad Sci USA **103:** 11417–11422

Bootten TJ, Harris PJ, Melton LD, Newman RH (2004) Solid-state ^{13}C-NMR spectroscopy shows that the xyloglucans in the primary cell walls of mung bean (*Vigna radiata* L.) occur in different domains: a new model for xyloglucan-cellulose interactions in the cell wall. J Exp Bot **55:** 571–583

Bradford MM (1976) A rapid and sensitive method for the quantitation of microgram quantities of protein utilizing the principle of protein-dye binding. Anal Biochem **72:** 248–254

Burton RA, Gidley MJ, Fincher GB (2010) Heterogeneity in the chemistry, structure and function of plant cell walls. Nat Chem Biol **6:** 724–732

Caffall KH, Mohnen D (2009) The structure, function, and biosynthesis of plant cell wall pectic polysaccharides. Carbohydr Res **344:** 1879–1900

Carpita N, Sabularse D, Montezinos D, Delmer DP (1979) Determination of the pore size of cell walls of living plant cells. Science **205:** 1144–1147

Cavalier DM, Lerouxel O, Neumetzler L, Yamauchi K, Reinecke A, Freshour G, Zabotina OA, Hahn MG, Burgert I, Pauly M, et al (2008) Disrupting two *Arabidopsis thaliana* xylosyltransferase genes results in plants deficient in xyloglucan, a major primary cell wall component. Plant Cell **20:** 1519–1537

Chanliaud E, Burrows KM, Jeronimidis G, Gidley MJ (2002) Mechanical properties of primary plant cell wall analogues. Planta **215:** 989–996

Chanliaud E, De Silva J, Strongitharm B, Jeronimidis G, Gidley MJ (2004) Mechanical effects of plant cell wall enzymes on cellulose/xyloglucan composites. Plant J **38:** 27–37

Cleland RE (1984) The Instron technique as a measure of immediate-past wall extensibility. Planta **160:** 514–520

Cosgrove DJ (1989) Characterization of long-term extension of isolated cell walls from growing cucumber hypocotyls. Planta **177:** 121–130

Cosgrove DJ (2005) Growth of the plant cell wall. Nat Rev Mol Cell Biol **6:** 850–861

Cregg JM, Cereghino JL, Shi J, Higgins DR (2000) Recombinant protein expression in *Pichia pastoris*. Mol Biotechnol **16:** 23–52

Dick-Pérez M, Zhang Y, Hayes J, Salazar A, Zabotina OA, Hong M (2011) Structure and interactions of plant cell-wall polysaccharides by two- and three-dimensional magic-angle-spinning solid-state NMR. Biochemistry **50:** 989–1000

Ding SY, Himmel ME (2006) The maize primary cell wall microfibril: a new model derived from direct visualization. J Agric Food Chem **54:** 597–606

Doblin MS, Pettolino F, Bacic A (2010) Plant cell walls: the skeleton of the plant world. Funct Plant Biol **37:** 357–381

Durachko DM, Cosgrove DJ (March 11, 2009) Measuring plant cell wall extension (creep) induced by acidic pH and by alpha-expansin. J Vis Exp **11:** http://dx.doi.org/10.3791/1263

Fry SC, Smith RC, Renwick KF, Martin DJ, Hodge SK, Matthews KJ (1992) Xyloglucan endotransglycosylase, a new wall-loosening enzyme activity from plants. Biochem J **282:** 821–828

Fry SC, York WS, Albersheim P, Darvill A, Hayashi T, Joseleau J-P, Kato Y, Lorences EP, Maclachlan GA, McNeil M, et al (1993) An unambiguous nomenclature for xyloglucan-derived oligosaccharides. Physiol Plant **89:** 1–3

Fujino T, Sone Y, Mitsuishi Y, Itoh T (2000) Characterization of cross-links between cellulose microfibrils, and their occurrence during elongation growth in pea epicotyl. Plant Cell Physiol **41:** 486–494

Gardner SL, Burrell MM, Fry SC (2002) Screening of Arabidopsis thaliana stems for variation in cell wall polysaccharides. Phytochemistry **60:** 241–254

Gloster TM, Ibatullin FM, Macauley K, Eklöf JM, Roberts S, Turkenburg JP, Bjørnvad ME, Jørgensen PL, Danielsen S, Johansen KS, et al (2007) Characterization and three-dimensional structures of two distinct bacterial xyloglucanases from families GH5 and GH12. J Biol Chem **282:** 19177–19189

Hamant O, Traas J (2010) The mechanics behind plant development. New Phytol **185:** 369–385

Harris PJ, Stone BA (2008) Chemistry and molecular organization of plant cell walls. *In* M Himmel, ed, Biomass Recalcitrance. Wiley-Blackwell, Hoboken, NJ, pp 61–93

Hartati S, Sudarmonowati E, Park YW, Kaku T, Kaida R, Baba K, Hayashi T (2008) Overexpression of poplar cellulase accelerates growth and disturbs the closing movements of leaves in sengon. Plant Physiol **147:** 552–561

Hayashi T (1989) Xyloglucans in the primary cell wall. Annu Rev Plant Physiol Plant Mol Biol **40:** 139–168

Hayashi T, Maclachlan G (1984) Pea xyloglucan and cellulose. I. Macromolecular organization. Plant Physiol **75:** 596–604

Hayashi T, Marsden MP, Delmer DP (1987) Pea xyloglucan and cellulose. VI. Xyloglucan-cellulose interactions *in vitro* and *in vivo*. Plant Physiol **83:** 384–389

Hestrin S, Schramm M (1954) Synthesis of cellulose by Acetobacter xylinum. II. Preparation of freeze-dried cells capable of polymerizing glucose to cellulose. Biochem J **58:** 345–352

Hsieh YS, Harris PJ (2009) Xyloglucans of monocotyledons have diverse structures. Mol Plant **2:** 943–965

Itoh T, Ogawa T (1997) Molecular architecture of the cell wall of poplar cells in suspension culture, as revealed by rapid-freezing and deep-etching techniques. Plant Cell Physiol **34:** 1187–1196

Kaku T, Tabuchi A, Wakabayashi K, Hoson T (2004) Xyloglucan oligosaccharides cause cell wall loosening by enhancing xyloglucan endotransglucosylase/hydrolase activity in azuki bean epicotyls. Plant Cell Physiol **45:** 77–82

Karlsson J, Siika-aho M, Tenkanen M, Tjerneld F (2002) Enzymatic properties of the low molecular mass endoglucanases Cel12A (EG III) and Cel45A (EG V) of *Trichoderma reesei*. J Biotechnol **99:** 63–78

Keegstra K, Talmadge KW, Bauer WD, Albersheim P (1973) The structure of plant cell walls. III. A model of the walls of suspension-cultured sycamore cells based on the interconnections of the macromolecular components. Plant Physiol **51:** 188–197

Knox JP (2008) Revealing the structural and functional diversity of plant cell walls. Curr Opin Plant Biol **11:** 308–313

Labavitch JM, Ray PM (1974) Relationship between promotion of xyloglucan metabolism and induction of elongation by indoleacetic acid. Plant Physiol **54:** 499–502

Lacayo CI, Malkin AJ, Holman HY, Chen L, Ding S-Y, Hwang MS, Thelen MP (2010) Imaging cell wall architecture in single *Zinnia elegans* tracheary elements. Plant Physiol **154:** 121–133

Lever M (1972) A new reaction for colorimetric determination of carbohydrates. Anal Biochem **47:** 273–279

Lopez-Casado G, Urbanowicz BR, Damasceno CM, Rose JK (2008) Plant glycosyl hydrolases and biofuels: a natural marriage. Curr Opin Plant Biol **11:** 329–337

Marcus SE, Verhertbruggen Y, Hervé C, Ordaz-Ortiz JJ, Farkas V, Pedersen HL, Willats WG, Knox JP (May 22, 2008) Pectic homogalacturonan masks abundant sets of xyloglucan epitopes in plant cell walls. BMC Plant Biol **8:** http://dx.doi.org/10.1186/1471-2229-8-60

McCann MC, Wells B, Roberts K (1990) Direct visualization of cross-links in the primary cell wall. J Cell Sci **96:** 323–334

McQueen-Mason S, Durachko DM, Cosgrove DJ (1992) Two endogenous proteins that induce cell wall extension in plants. Plant Cell **4:** 1425–1433

McQueen-Mason SJ, Fry SC, Durachko DM, Cosgrove DJ (1993) The relationship between xyloglucan endotransglycosylase and in-vitro cell wall extension in cucumber hypocotyls. Planta **190:** 327–331

Nishitani K, Masuda Y (1983) Auxin-induced changes in the cell wall xyloglucans: effects of auxin on the two different subtractions of xyloglucans in the epicotyl cell wall of *Vigna angularis*. Plant Cell Physiol **24:** 345–355

Nishitani K, Tominaga R (1992) Endo-xyloglucan transferase, a novel class of glycosyltransferase that catalyzes transfer of a segment of xyloglucan molecule to another xyloglucan molecule. J Biol Chem **267:** 21058–21064

Park YB, Cosgrove DJ (2012) Changes in cell wall biomechanical properties in the xyloglucan-deficient *xxt1/xxt2* mutant of Arabidopsis. Plant Physiol **158:** 465–475

Park YW, Tominaga R, Sugiyama J, Furuta Y, Tanimoto E, Samejima M, Sakai F, Hayashi T (2003) Enhancement of growth by expression of poplar cellulase in *Arabidopsis thaliana*. Plant J **33:** 1099–1106

Pauly M, Albersheim P, Darvill A, York WS (1999) Molecular domains of the cellulose/xyloglucan network in the cell walls of higher plants. Plant J **20:** 629–639

Saladié M, Rose JK, Cosgrove DJ, Catalá C (2006) Characterization of a new xyloglucan endotransglucosylase/hydrolase (XTH) from ripening tomato fruit and implications for the diverse modes of enzymic action. Plant J **47:** 282–295

Sandgren M, Stahlberg J, Mitchinson C (2005) Structural and biochemical studies of GH family 12 cellulases: improved thermal stability, and ligand complexes. Prog Biophys Mol Biol **89:** 246–291

Scheller HV, Ulvskov P (2010) Hemicelluloses. Annu Rev Plant Biol **61:** 263–289

Schopfer P (2006) Biomechanics of plant growth. Am J Bot **93:** 1415–1425

Shani Z, Dekel M, Tsabary G, Goren R, Shoseyov O (2004) Growth enhancement of transgenic poplar plants by overexpression of *Arabidopsis thaliana* endo-1,4-β-glucanase (*cel1*). Mol Breed **14:** 321–330

Somerville C, Bauer S, Brininstool G, Facette M, Hamann T, Milne J, Osborne E, Paredez A, Persson S, Raab T, et al (2004) Toward a systems approach to understanding plant cell walls. Science **306:** 2206–2211

Talbott LD, Ray PM (1992) Changes in molecular size of previously deposited and newly synthesized pea cell wall matrix polysaccharides: effects of auxin and turgor. Plant Physiol **98:** 369–379

Thimm JC, Burritt DJ, Ducker WA, Melton LD (2000) Celery (*Apium graveolens* L.) parenchyma cell walls examined by atomic force microscopy: effect of dehydration on cellulose microfibrils. Planta **212:** 25–32

Van Sandt VS, Suslov D, Verbelen JP, Vissenberg K (2007) Xyloglucan endotransglucosylase activity loosens a plant cell wall. Ann Bot (Lond) **100:** 1467–1473

Whitney SE, Wilson E, Webster J, Bacic A, Reid JSG, Gidley MJ (2006) Effects of structural variation in xyloglucan polymers on interactions with bacterial cellulose. Am J Bot **93:** 1402–1414

Yuan S, Wu Y, Cosgrove DJ (2001) A fungal endoglucanase with plant cell wall extension activity. Plant Physiol **127:** 324–333

Zhao Q, Yuan S, Wang X, Zhang Y, Zhu H, Lu C (2008) Restoration of mature etiolated cucumber hypocotyl cell wall susceptibility to expansin by pretreatment with fungal pectinases and EGTA in vitro. Plant Physiol **147:** 1874–1885

Zykwinska AW, Ralet MC, Garnier CD, Thibault JF (2005) Evidence for in vitro binding of pectin side chains to cellulose. Plant Physiol **139:** 397–407